Electronic Supplementary Information

Anisotropy nonvolatile magnetization controlled by electric field in amorphous SmCo thin films grown on (011)-cut PMN-PT substrates

Wenhui Liang,[a,b] Fengxia Hu,[*a,b,c] Jian Zhang,[*d] Hao Kuang,[a,b] Jia Li,[a,b] Jiefu Xiong,[a,b] Jing Wang,[*a,b,e] Kaiming Qiao,[a,b] Jirong Sun,[a,b,c] and Baogen Shen[a,b,c]

[a] Beijing National Laboratory for Condensed Matter Physics and State Key Laboratory of Magnetism, Institute of Physics, Chinese Academy of Sciences, Beijing 100190, P. R. China

[b] School of Physical Sciences, University of Chinese Academy of Sciences, Beijing 100190, P. R. China

[c] Songshan Lake Materials Laboratory, Dongguan, Guangdong 523808, P. R. China

[d] Key Laboratory of Magnetic Materials and Devices, Ningbo Institute of Materials Technology and Engineering, Chinese Academy of Sciences, Ningbo 315201, China

[e] Fujian Institute of Innovation, Chinese Academy of Sciences, Fuzhou, Fujian 350108, P. R. China

[*]e-mail: fxhu@iphy.ac.cn, zhangj@nimte.ac.cn, wangjing@iphy.ac.cn

S1. Electric-field-induced polarization switching in R phase and the rhombohedral-orthorhombic (R-O) phase transformation for (011)-poled PMN-PT single crystals.

The polarization switching in R phase, on the whole, can be divided into two categories, 180° polarization switching ($r1^+ \rightarrow r1^-$ or $r2^+ \rightarrow r2^-$) and non-180° polarization switching (Figure S1). Specifically, non-180° polarization switching can be subdivided into two types, 71° polarization switching ($r1^+ \rightarrow r3^+/r4^+$ or $r2^+ \rightarrow r3^-/r4^-$) and 109° polarization switching ($r1^+ \rightarrow r3^-/r4^-/r2^-$ or $r2^+ \rightarrow r3^+/r4^+/r1^-$).[1] As the preferential polarization directions of PMN-PT change from out-of-(011)-plane (i.e., $r1^+$ and $r2^+$) to the four possible in-plane <111> directions, both 71° and 109°, namely, non-180°, polarization switching occur (left hand in Figure S1).

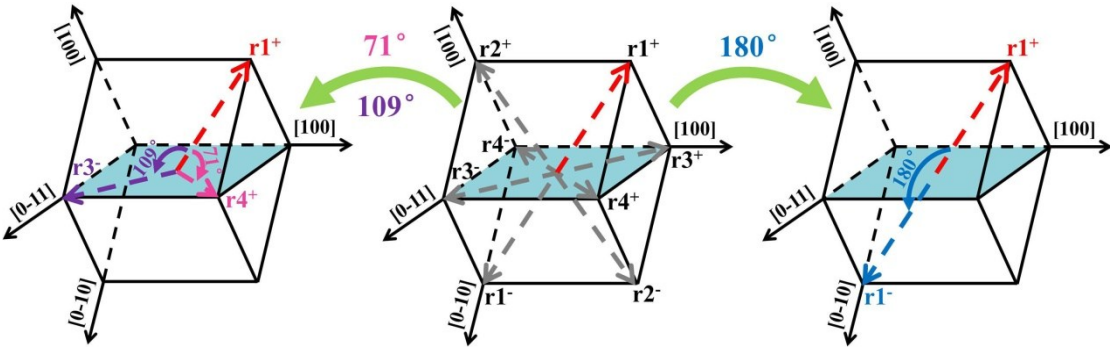

Figure S1. The different types of polarization switching in R phase. $r1^+/r1^-/ r2^+/r2^-/ r3^+/ r3^-/ r4^+/ r4^-$ represent the 8-possible <111> polarization directions.

For the (1-x)PMN-xPT single crystals near the MPB (x=0.28-0.32), R-O phase transition can be induced by an electric field, E.[2-4] It has been observed that the numerical value of critical E monotonously decreases from ~10 kV/cm to ~2 kV/cm with increasing PT concentration from x = 0.28 to 0.32, and irreversible R-O phase transition and strain memory effect occurs at x = 0.32.[2] Although the commercial (1-x)PMN-xPT substrate used in present work has a nominal composition around x ~ 0.30, the possibility of component inhomogeneity may lead to different critical E. In other words, within ±8 kV/cm, part of R phase may remain stable and non-180° (71° and 109°) polarization switching contributes to the butterfly-like behavior, while the other part contributes to the loop-like behavior owing to the irreversible R-O phase transition induced by E.[2] Separating the Mr-E curves into symmetric butterfly-like and antisymmetric loop-like parts provides a clear expression, as shown in Figures 3 (b) and (c). Moreover, the electric field induced polarization switching and R-O phase transition has been illustrated in Figure S2.

On the one hand, the evolutionary process of polarization directions in R phase as the electric field changes from +0 kV/cm to -0 kV/cm (+0 ~ $-E_{cr}$ ~ -8 ~ -0 kV/cm) is shown in Figures S2a-d. During the application of -8 kV/cm (A_1-B_1-C_1 in Figure 3b), the preferential polarization directions of the substrate change from [-111] and [111] (Figure S2a, point A_1 in Figure 3b) to the four possible in-plane <111> directions (Figure S2b, point B_1 in Figure 3b), and then rotate to [1-1-1] and [-1-1-1] (Figure

S2c, point C_1 in Figure 3b). In this process, the compressive strain along [100] direction decreases firstly and then increases, and the turning point lies in the coercive field E_{cr} (Figure S2b, point B_1 in Figure 3b). After that, when the electric field is removed from point C_1 to D_1 (Figure 3b), the domain structure at point D_1 (Figure S2d) remains basically the same as that at point C_1 ([1-1-1], [-1-1-1]). However, the emergence of a few proportions of the non-180° (71° and 109°) polarization switching cannot be excluded during the decreasing procession of the electric field,[2] so that the compressive strain at -0 kV/cm (Figure S2d, point D_1 in Figure 3b) is not as large as that at -8 kV/cm (Figure S2c, point C_1 in Figure 3b). Moreover, when the electric field is applied reversely (D_1-E_1-F_1-A_1 in Figure 3b), the variation tendency of compressive strain remains similar while the direction of polarization is just the opposite. To avoid repetition, the schematics are no longer given, and the details won't be described any more.

On the other hand, the evolutionary process of the domain structure in R-O phase transformation as the electric field changes from +0 kV/cm to -0 kV/cm (+0 ~ -8 ~ -0 kV/cm) is illustrated in Figures S2e-h. The same as that shown in Figure S2a, the two preferential polarization directions ([-111], [111]) of R phase (Figure S2e) rotate towards [011] direction of O phase (Figure S2f) when the electric field increases from +0 to -8 kV/cm. The strain along in-pane [100] direction induced by the R-O phase transformation is also compressive and the amplitude is even larger than the strain induced by the polarization switching in the R phase. This O phase remains almost unchanged even the electric field of -8 kV/cm is removed (Figure S2g to h, point C_2 to D_2 in Figure 3c), and so does the compressive strain, hence resulting in the nonvolatile regulation and the two states of M_r at +0 kV/cm and -0 kV/cm (point A_2, D_2 in Figure 3c). When a positive electric field is applied (-0 ~ +8 ~ +0 kV/cm, point D_2-F_2-A_2 in Figure 3c), the substrate returns to R phase and remains unchanged even the electric field decreases to +0 kV/cm. Though the strain in this procession (O-R phase transformation) is still compressive, the strain releases, rather than strain accumulates.

In summary, for the process of applying negative electric fields (+0 ~ -E_{cr} ~ -8 ~ -0 kV/cm), especially from –E_{cr} to -8 kV/cm, the non-180° (71° and 109°) polarization switching in R phase leads to the accumulation of compressive strain along in-pane [100] direction, while the R-O phase transformation makes the compressive strain go up. The combination of the two leads to the maximum compressive strain at point C in Figure 3a. Nevertheless, when a positive electric field is applied (D-E-F, Figure 3a), the butterfly-like part accumulates the compressive strain (D_1-E_1-F_1, Figure 3b) on the whole, while the loop-like part releases the compression (D_2-F_2, Figure 3c). It means that the latter is a drag on the comprehensive compressive strain, which results in the smaller compressive strain at point F than that at point C (Figure 3a).

What needs to be explained is that on the variation of the electric field, the tendency of the strain along [01-1] direction is the same as that along [100] direction. The difference is that the latter is compressive while the former is tensile. The variety of the tensile strain is also induced by the polarization switching in R phase, as well as

the irreversible R-O phase transformation, and the details won't be discussed further.

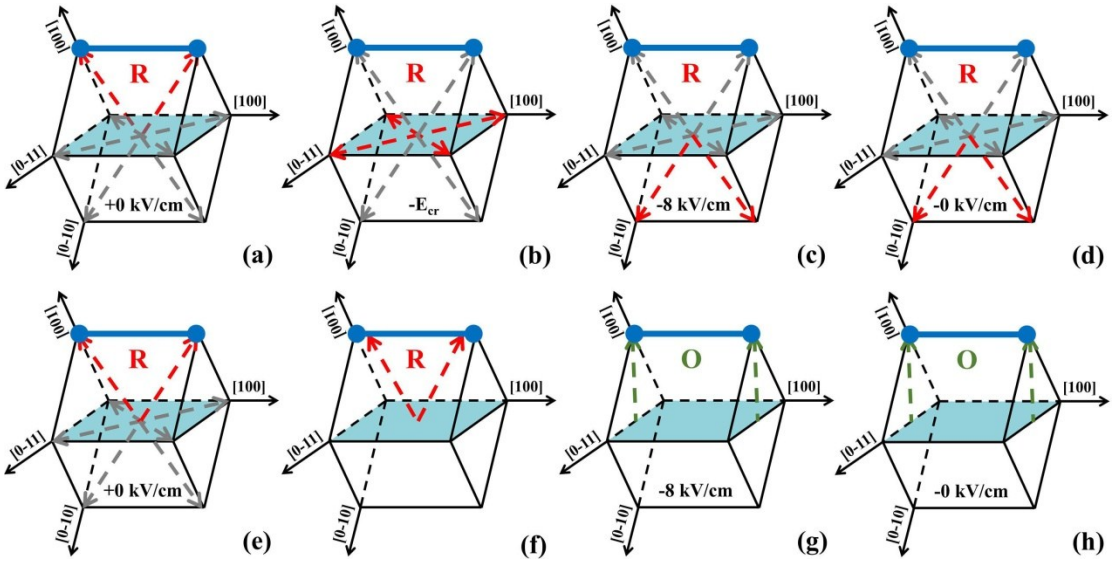

Figure S2. The polarization switching in R phase and the R-O phase transformation with the electric field changes from +0 kV/cm to -0 kV/cm (+0 ~ -8 ~ -0 kV/cm). Schematics of domain structures during (a-d) the polarization switching in R phase, and (e-h) R-O phase transformation, where Figure S2e represents the possible intermediate state from R to O phase. The overstriking blue lines highlight the [100] direction.

S2. X-ray diffraction (XRD) patterns and x-ray diffraction reciprocal space mappings (XRD-RSM) of (011)-PMN-0.3PT single crystals with in situ electric fields applied along the [011] direction.

Figure S3 shows the XRD patterns around (011) peak for (011)-oriented PMN-0.3PT single crystals under different electric fields. When the electric field is +0 kV/cm (Figure S3a), only the (011) peak of R phase can be detected. As the electric field increases to -8 kV/cm (Figure S3b), two peaks appear. The left one is identified to be the (011) peak of O phase according to the peak position[3], while the right one still comes from the R phase. The left shift of the R(011) peak (Figure S3b) compared to Figure S3a indicates the elongation of lattice along out-plane [011] direction, which is in line with the compression along in-plane [100] and the resulted enhancement of Mr in R phase (see Figure 3b, A_1-B_1-C_1). When the electric field is removed from -8 kV/cm to -0 kV/cm (Figure S3b to Figure S3c), the two peaks remain, and the peak position from O phase keeps nearly unchanged, strongly demonstrating the memory effect of stress and Mr (see Figure 3c, C_2-D_2). Meanwhile, the R(011) peak returns and moves right, indicating the release of the tensile strain along out-plane [011], which is also in line with the release of compression along in-plane [100] and the reduction of Mr in R phase (see Figure 3b, C_1-D_1). Besides, it can be found that the R(011) peak becomes broadened, which may probably due to the incomplete switching of the polarizations. After that, when the electric field is increased from -0

kV/cm to +8 kV/cm (Figure S3c to Figure S3d), the R phase dominates while a little O phase coexists (in line with Figure 3c, D_2-F_2), and the R(011) peak shifts left, indicating the elongation of lattice along out-plane [011] direction, which also agrees with the compression along in-plane [100] direction and the resulted enhancement of Mr in R phase (see Figure 3b, D_1-E_1-F_1). The existence of the small part of residual O phase at +8 kV/cm may origin from the incompletion of the O-R phase transformation. After the +8 kV/cm was removed (Figure S3e), the R phase almost returns to that shown in Figure S3a, demonstrating the release of the tensile strain along out-plane [011], which is also consistent with the release of compression along in-plane [100] and the reduction of Mr in R phase (see Figure 3b, F_1-A_1). All these XRD results verify the R-O phase transition induced by electric field and possible coexistence of stable and unstable R phase. The latter transforms to O phase under electric field while polarization switching occurs for the former.

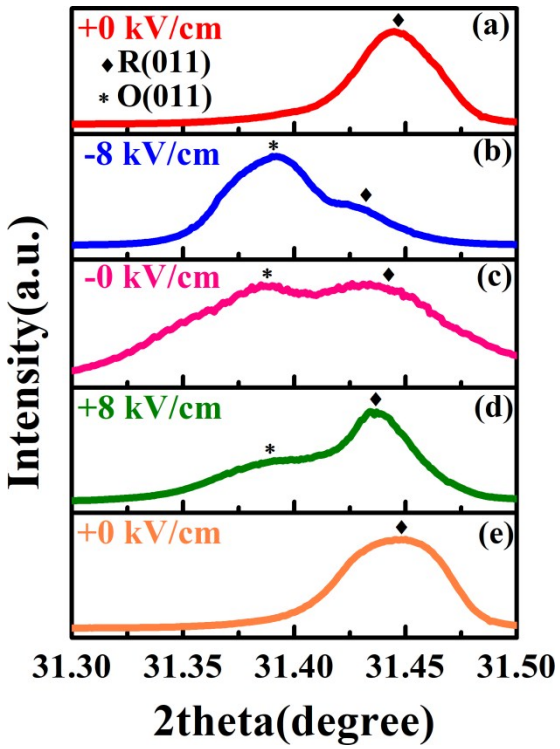

Figure S3. The X-ray diffraction patterns of (011)-oriented PMN-0.3PT single crystals with in situ electric field applied in the sequence of (a) +0 kV/cm, (b) -8 kV/cm, (c) -0 kV/cm, (d) +8 kV/cm , (e) +0 kV/cm along the [011] direction.

To give more evidences of the R-O phase transition, we measured x-ray diffraction reciprocal space mappings (XRD-RSMs) under in situ electric fields, which are presented in Figure S4. The asymmetrical R-O phase transition can be clearly identified from the RSMs.

Figure S4 shows the XRD-RSMs around the (-222) reflection of (011)-oriented PMN-0.3PT single crystals under different in-situ electric fields. When the electric field is at +0 kV/cm (Figure S4a), only R phase appears. As -8 kV/cm was applied, three spots appear (Figure S4b). The right top two correspond to R phase while the

left bottom one corresponds to O phase, evidencing the electric field-induced R-O phase transformation and the coexistence of R and O phase at -8 kV/cm. When the electric field is removed from -8 kV/cm to -0 kV/cm (Figure S4b to Figure S4c), the spot corresponding to O phase remains and it still coexists with R phase, strongly evidencing the irreversible R-O phase transition and the memory effect of stress and Mr (corresponding to Figure 3c, C_2-D_2). After that, when the electric field is increased from -0 kV/cm to +8 kV/cm (Figure S4c to Figure S4d), the spots corresponding to R phase dominate while the O phase becomes very weak (in line with Figure 3c, D_2-F_2). In this process, O-R phase transformation occurs. After the +8 kV/cm is decreased to +0 kV/cm, R phase still dominates and O phase nearly vanishes (Figure S4a). This process is completely in line with the θ-2θ XRD results (Figure S3) and supports the dependence of Mr on E (Figure.3).

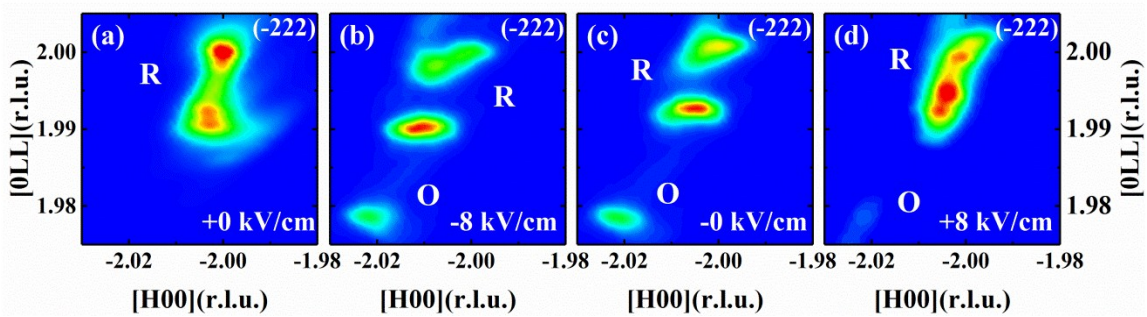

Figure S4. The X-ray diffraction reciprocal space mappings around the (-222) reflection of (011)-oriented PMN-0.3PT single crystals with in situ electric field applied of (a) +0 kV/cm, (b) -8 kV/cm, (c) -0 kV/cm, (d) +8 kV/cm along the [011] direction.

S3. The dependence of strain on electric field (strain-E curves) for the two in-plane directions and P-E curve of PMN-PT.

To understand the magnetization controlled by electric fields in amorphous SmCo thin films grown on the (011)-cut PMN-PT substrates, the strain-electric field curves and P-E curve are measured and presented in Figure S5.

Figure S5a shows the dependence of strain on electric field (strain-E curves) along the two in-plane directions. Similar to the Mr-E curves (Figure 3a and Figure 6a), the strain-electric field curves (Figure. S5a) are also asymmetric for the positive and negative electric fields due to the superposition of the polarization reorientation in R phase and the irreversible R-O phase transition. When the negative electric field is applied (point A-B-C), the compressive strain along [100] direction decreases firstly and then increases, and finally reaches the maximum at point C. After that, with decreasing electric field along path C-D, the compressive strain nearly reduces all the way. Later on, with applying positive electric fields (D-E-F-A), a similar situation prevails—the trends of strain with the variation of electric field remain similar. However, the changes in strain under the positive electric fields are much smaller than those under the negative ones owing to the following cause. When a positive electric

field is applied (D-E-F), the polarization reorientation of R phase brings about the accumulation of compression on the whole, while the R-O phase transformation leads to the relief of the compression. It means that the latter is a drag on the comprehensive compressive strain, which would result in the smaller compressive strain compared to the negative electric fields. The variation tendency of the strain along [01-1] is just the opposite and the details would not be repeated here. Besides, the strain-E curves from Ecr to maximum electric field (B-C) and from maximum electric field to zero (C-D) are not as smooth as those in Mr-E curves. The reason is still not clear at the moment.

Figure S5b shows a polarization-electric field (P-E) curve of PMN-PT measured at room temperature with a frequency of 1kHz. The measurement was operated on the capacitance configuration using Radiant ferroelectric tester Premier II. One can notice the different residual polarization Pr at +0 kV/cm (A) and -0 kV/cm (D), and the different coercivity fields at points B and E. This phenomenon accords with the asymmetric Mr-E (Figure 3a and Figure 6a) and strain-E (Figure S5a) curves. When the electric field is +0 kV/cm (point A), PMN-PT is in R phase. After that, when the negative electric field is applied (point A-B-C), both R-O phase transition and polarization reorientation of R phase occur. Not only R phase, but also O phase coexists at point C. When the electric field is removed from point C to D, O phase still exists due to the irreversibility of the R-O phase transition, i.e. memory effect. The polarization contributed by R phase rotates, while the polarization contributed by O phase remains at point D. Hence, Pr at -0 kV/cm (point D) is bigger than that at +0 kV/cm (point A). When an electric field of +8 kV/cm (point D-E-F) is applied, O-R phase transition occurs and R phase dominates at point F. This O-R phase transition has an effect on the coercive field and leads to the difference of E_{cr} at point B and E, which also accords with the asymmetric Mr-E (Figure 3a and Figure 6a) and strain-E (Figure S5a) curves.

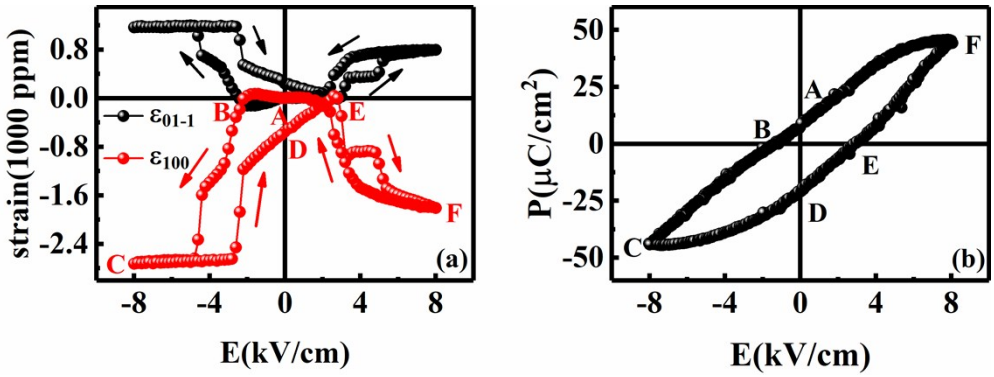

Figure S5. (a) The dependence of strain on electric field (strain-E curves) for the two in-plane directions. (b) P-E curve of PMN-PT. To avoid confusion, the letters (A/B/C/D/E/F) here represent the same electric fields as those in Figure S5(a).

References

1 B. Peng, C. Zhang, Y. Yan, M. Liu, *Phys. Rev. A,* 2017**, 7,** 044015.

2 P. Zhao, M. Bao, A. Bur, J. L. Hockel, K. Wong, K. P. Mohanchandra, C. S. Lynch, G. P. Carman, *J. Appl. Phys.* , 2011**, 109**, 124101.

3 M. Shanthi, S. M. Chia, L. C. Lim, *Appl. Phys. Lett.*, 2005**, 87,** 202902.

4 M. Shanthi, L. C. Lim, *J. Appl. Phys.,* 2009, **106**, 114116.

5 M. Shanthi, L. C. Lim, *Appl. Phys. Lett.*, 2009**, 95,** 102901.